ELSEVIER

Journal of Alloys and Compounds 469 (2009) 207–214

Journal of ALLOYS AND COMPOUNDS

www.elsevier.com/locate/jallcom

Solid-state and liquid-state interfacial reactions between Sn-based solders and single crystal Ag substrate

H.F. Zou, Z.F. Zhang *

Shenyang National Laboratory for Materials Science, Institute of Metal Research, Chinese Academy of Science, Shenyang 110016, PR China

Received 24 October 2007; received in revised form 16 January 2008; accepted 18 January 2008
Available online 4 March 2008

Abstract

Growth kinetics and interfacial morphologies of the intermetallic compounds (IMCs) between single crystal Ag and Sn–4Ag, Sn–3Cu and Sn–37Pb solders were investigated by solid-state aging at 160 °C and liquid-state aging at 260 °C. Isothermal equation of chemical reaction and phase diagrams were used to explain the effects of Ag, Cu and Pb on the growth kinetics of IMCs under solid-state and liquid-state aging conditions. The diffusion coefficients for the three solder joints of Sn–4Ag/Ag, Sn–3Cu/Ag and Sn–37Pb/Ag were calculated after solid-state and liquid-state aging. It is found that Pb can effectively retard the growth of IMCs during liquid-state aging but has little influence on the growth rate of IMCs during the solid-state aging. Some local small cracks were frequently observed in the Cu_6Sn_5 particles near interfaces of the Sn–3Cu/Ag solder joints after solid-state aging for several days. However, there were no such local small cracks when solders or interfaces did not contain the Cu_6Sn_5 particles after the same aging time.
© 2008 Elsevier B.V. All rights reserved.

Keywords: Ag single crystal substrate; Lead-free solder; Intermetallic compounds (IMCs); Growth kinetics; Local cracks

1. Introduction

In the electronic packaging field, there are two kinds of jointing methods, i.e., brazing and soldering. Brazing is the joining of metals through heating a filler metal, whose melting point is above 450 °C but below the melting point of the jointed metal. Soldering is that two metals are joined together by means of a third metal or alloy having a relatively low melting point. Therefore, soldering joints will produce some intermetallic compounds (IMCs) at the interface; whereas brazing joints mainly involve solid solutions without the IMCs. Normally, solders supply electrical, thermal and mechanical continuity [1]. During the soldering procedure, the molten solders react with the substrates, resulting in the formation of IMCs with several microns thick between solders and the substrate interface [2,3]. Therefore, no matter whether there are Sn–Pb solders or lead-free solders, their interfacial reactions often play an important role in the joint properties, such as mechanical properties.

In the past, the traditional Sn–Pb alloys were widely used as important solders due to low cost, good solderability, low melting point and reliable interfacial bonding [4]. However, many countries such as USA, Japan and EU members prohibit the use of Pb and its compounds in the electrical packaging industry because Pb is identified as one of the most toxic chemicals to the human body. In order to eliminate Sn–Pb solders, great efforts have been devoted to develop new kinds of lead-free solders [5–10]. Among several lead-free candidate alloys, the eutectic and near eutectic Sn–Ag and Sn–Cu alloys are the most promising to replace the Sn–Pb solders in future electronic packaging [3,11–15]. In addition to the composition of the solder, the substrate is also crucial for the solder reliability because the substrate always takes part in the interfacial reaction. For example, a Ni layer is widely used to retard the growth of IMCs during solid-state and liquid-state aging. No matter whether the substrate is Ni or Cu, the interfacial reaction product is more than one layer IMC. For a Ni substrate, the IMCs may be Ni_3Sn, Ni_3Sn_2 or Ni_3Sn_4 phases; Cu_3Sn and Cu_6Sn_5 phases often appear between copper substrate and Sn-based solders [2,3,8,16,17]. It is better to reduce the formation of multiple layers of IMCs in the soldering interfaces because the brittle IMCs often have harmful influences on the mechanical properties of the soldering joints

* Corresponding author. Tel.: +86 24 23971043; fax: +86 24 23891320.
E-mail address: zhfzhang@imr.ac.cn (Z.F. Zhang).

0925-8388/$ – see front matter © 2008 Elsevier B.V. All rights reserved.
doi:10.1016/j.jallcom.2008.01.082

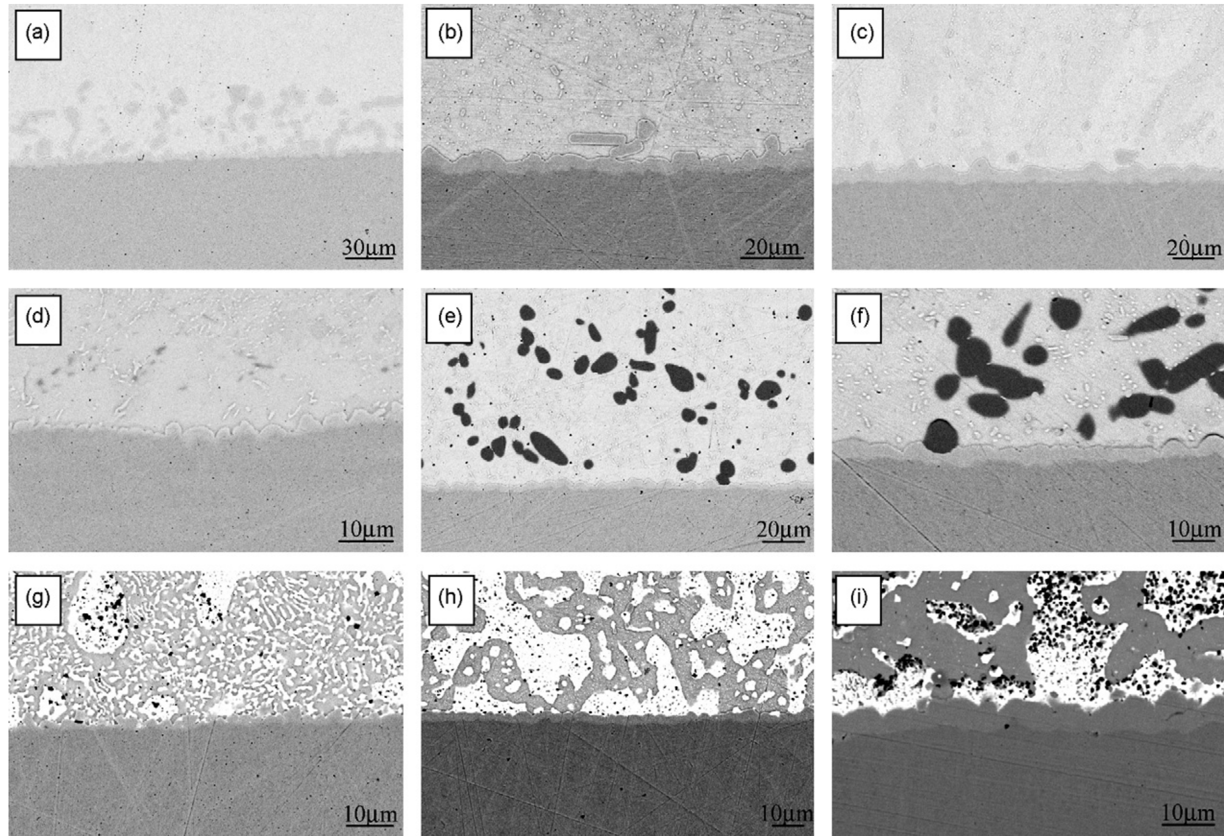

Fig. 1. SEM micrographs of the Ag_3Sn IMC between the three solders and single crystal Ag substrate after aging at 160 °C for different time: (a) as reflowed, (b) aging for 3 days and (c) 11 days for Sn–4Ag/Ag; (d) as reflowed, (e) aging for 3 days and (f) 11 days for Sn–3Cu/Ag; (g) as reflowed, (h) aging for 3 days and (i) 11 days for Sn–37Pb/Ag.

[8]. Among several pure metals with good conductivity, it is found that Ag is a suitable substrate to form only one layer IMC (Ag_3Sn) after chemical reactions with most Sn-based solders [2,18,19]. It is expected that the simple interfacial reaction between Ag and the solders will be beneficial to the soldering joint reliability [2,18,19]. However, there are limited data available about the interfacial reactions and the growth kinetics of the IMC between Ag and lead-free solders [18–20]. In this research, the interfacial reactions of Ag and three typical solders, i.e., Sn–4Ag, Sn–3Cu and Sn–37Pb, were investigated. Isothermal equations of chemical reaction and phase diagrams were employed to explain the effects of Ag, Cu and Pb on the growth kinetics of the IMCs for the solid-state and liquid-state aging heat treatments. In order to avoid the potential influences of grain boundaries and crystallographic orientations, single crystal Ag was used as substrate in this research.

2. Experimental procedure

In this study, single crystal Ag was used as a substrate and Sn–4Ag, Sn–3Cu and Sn–37Pb alloys were employed as solders. Firstly, single crystal Ag plate with a dimension of 40 mm × 80 mm × 10 mm was grown from Ag with a purity of 99.999% by the Bridgman method in a horizontal furnace. Secondly, the three kinds of solders were prepared by melting high purity (4N) Sn and Ag, Sn and Cu, Sn and Pb in vacuum ($<10^{-1}$ Pa) at 800 °C for 30 min. The single crystal Ag and the solders were ground with 800#, 1000#, 2000# SiC paper and then carefully polished with 2.5, 1.5 and 0.5 μm polishing pastes. Next, the samples were ultrasonically cleaned in ethanol for 10 min after polishing. In order to make the interfacial reactions occur under the same conditions, the three kinds of solders were put onto the same piece of single crystal Ag. Some

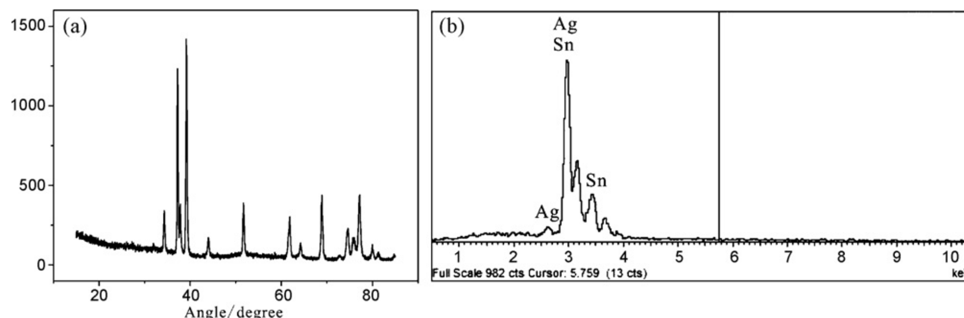

Fig. 2. (a) XRD of the Ag_3Sn and (b) element spectrum of Ag_3Sn.

rosin mildly activated (RMA) flux was employed on the surface of solders and substrates. Finally, the prepared samples were bonded in the oven with a constant temperature of 240 °C for several minutes. After the reflowing of the solders with the Ag substrate, they were firstly observed by scanning electron microscope (SEM) to check the cross-section. Then, one group of as-reflowed samples was isothermally aged at 160 °C for 0, 1, 3, 7, 11, and 15 days in order to study the IMC growth kinetics during solid-state aging. Another group of as-reflowed samples was isothermally aged at 260 °C for 0, 0.5, 1.5, 5, and 9 h to study the IMCs growth kinetics of the liquid-state aging. After solid-state and liquid-state aging, all samples were observed with a LEO super35 or a Cambridge S360 SEM to determine the morphology, composition and thickness of the interfacial IMCs. In order to better reveal the morphology of the reaction phases between the Ag substrate and the different solders, some samples after liquid-state aging were deeply etched with a 5% HCl + 3% HNO_3 + CH_3OH (wt%) etchant solution to remove the excess Sn phase so that the reaction phases can be exposed.

3. Results and discussion

3.1. The solid-state interfacial reaction

Fig. 1 shows SEM micrographs of the interfaces between Sn–4Ag, Sn–3Cu and Sn–37Pb solders and the single crystal Ag substrate isothermally aged at 160 °C for different periods. Fig. 2 shows the energy dispersive X-ray spectroscopy (EDS) analysis and XRD pattern of the IMC, it can be seen that only one IMC (Ag_3Sn) layer exists at the interfaces, and no Cu or Pb atoms were detected in any of the interfacial layers. Besides, the Ag_5Sn phase was not detected in any of the aged samples. These results are consistent with previous observations [2,18,19], indicating that the Ag_3Sn is the unique IMC phase forming on Ag substrates during aging.

Because IMCs always grow continuously with increasing aging time, it is necessary to measure the thickness of the IMCs between Ag and different solders. In this research, in order to decrease the error (method I), both the integral area and the length of IMCs layers were measured using a kind of special software (SISC IAS V 8.0). For example, the average thickness of the IMCs can be calculated by using the following equation:

$$z = \frac{S}{L_0} \quad (1)$$

Here L_0 is the length of the measured region, S is the integral contour area of the IMC at the interface, and z is the average thickness of the IMC layer. The average thickness of the IMCs can be also calculated by using the following equation (method II):

$$z = \frac{z_1 + z_2 + z_3 + \cdots + z_n}{n} \quad (2)$$

where $z_1, z_2, z_3, \ldots, z_n$ are the thicknesses of the IMC at different places of the interface. Fig. 3 demonstrates the dependence of the IMC thickness on the aging time at 160 °C. It can be seen that the thicknesses of the IMCs for the three solders are approximately proportional to the square root of the aging time, indicating that the growth of the Ag_3Sn layer is mainly controlled by diffusion. Accordingly, the diffusion coefficient can be calculated according to the following empirical equation [21]:

$$z = D^{1/2}\sqrt{t} + c \quad (3)$$

where z, t, D, c are the average thickness of the Ag_3Sn layer, the aging time, the diffusion coefficient and a constant, respectively. According to Eq. (3) and the data in Fig. 3, the diffusion coefficients D of Ag atoms and Sn atoms were calculated and follow an increasing order, i.e., 0.98×10^{-17}, 1.12×10^{-17}, $2.15 \times 10^{-17}\ m^2\,s^{-1}$, for Sn–4Ag, Sn–37Pb and Sn–3Cu solders, respectively (1.04×10^{-17}, 1.0×10^{-17}, $1.58 \times 10^{-17}\ m^2\,s^{-1}$ for method II). The current results are smaller than the previous results obtained in Sn–Ag–Cu/Cu joints, for example, $7.24 \times 10^{-17}\ m^2\,s^{-1}$ for aging at 170 °C [21], $4.7 \times 10^{-17}\ m^2\,s^{-1}$ for aging at 125 °C [22]. This indicates that the IMC growth rate between Ag substrates and solders is less than that between Cu substrate and solders.

As shown in Figs. 1 and 3, there are several differences in the morphology and thickness of the IMC layer for the three solder joints. Firstly, for the as-reflowed solder joints, the IMC layer of the Sn–4Ag/Ag joint is the thickest while the IMC of Sn–37Pb/Ag joint is the thinnest. It is well-known that the interfacial reaction between liquid Sn-based solder and Ag substrate can be described as

$$3Ag(l) + Sn(l) \rightarrow Ag_3Sn(s) \quad (4)$$

According to isothermal equation of chemical reaction [23]:

$$\Delta G = \Delta G^\circ + RT \ln \frac{\alpha_{Ag_3Sn}}{\alpha_{Sn}\alpha_{Ag}^3} \quad (5)$$

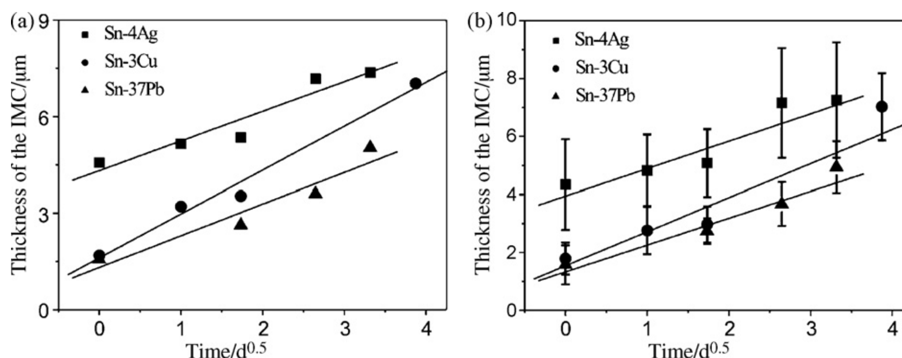

Fig. 3. Plot of the thickness of the Ag_3Sn layer vs. the square root of aging days for different solders aging at 160 °C; (a) method I, (b) method II.

As we know, Ag_3Sn is a solid phase and can be obtained:

$$\alpha_{Ag_3Sn} = 1, \quad \alpha_{Sn} = \gamma_{Sn}[Sn], \quad \alpha_{Ag} = \gamma_{Ag}[Ag] \tag{6}$$

Therefore, one can get

$$\Delta G = \Delta G^{\circ} + RT \ln \frac{1}{\gamma_{Sn}[Sn]\gamma_{Ag}^{3}[Ag]} \tag{7}$$

where ΔG and ΔG° are the Gibbs function of molar reaction and the standard Gibbs function of molar reaction, R is the gas constant, T is the absolute temperature, α_{Ag_3Sn}, α_{Sn}, α_{Ag} are the activities of Ag_3Sn, Ag atom and Sn atom in molten solder, γ_{Sn}, γ_{Ag} are the activity coefficients of Sn atom and Ag atom, [Sn], [Ag] are the concentrations of Sn and Ag atoms, respectively. In the following discussion, it is assumed that the values of γ_{Sn} and γ_{Ag} remained approximately constant in different liquid solders. Therefore in Eq. (7), it is apparent that the concentration of Ag atom plays a more important role in the formation of Ag_3Sn than the concentration of Sn atoms. With increasing concentration of Ag atoms, the ΔG will intensely decrease, leading to much easier reaction between Ag and Sn atoms. For the molten Sn–4Ag solder, the Sn atoms can react either with the Ag atoms in the Sn–4Ag solder or the Ag substrate. For Sn–37Pb solder, the Ag atoms will be prevented from going into the Sn–Pb system because the Ag–Pb system is immiscible. Although Sn–3Cu solder does not prevent the Ag atom from immersing into the solder to react with the Sn atoms, there are no Ag atoms in the Sn–3Cu solder at the beginning of the interfacial reaction. In other words, the concentration of [Ag] for the as-reflowed samples should follow

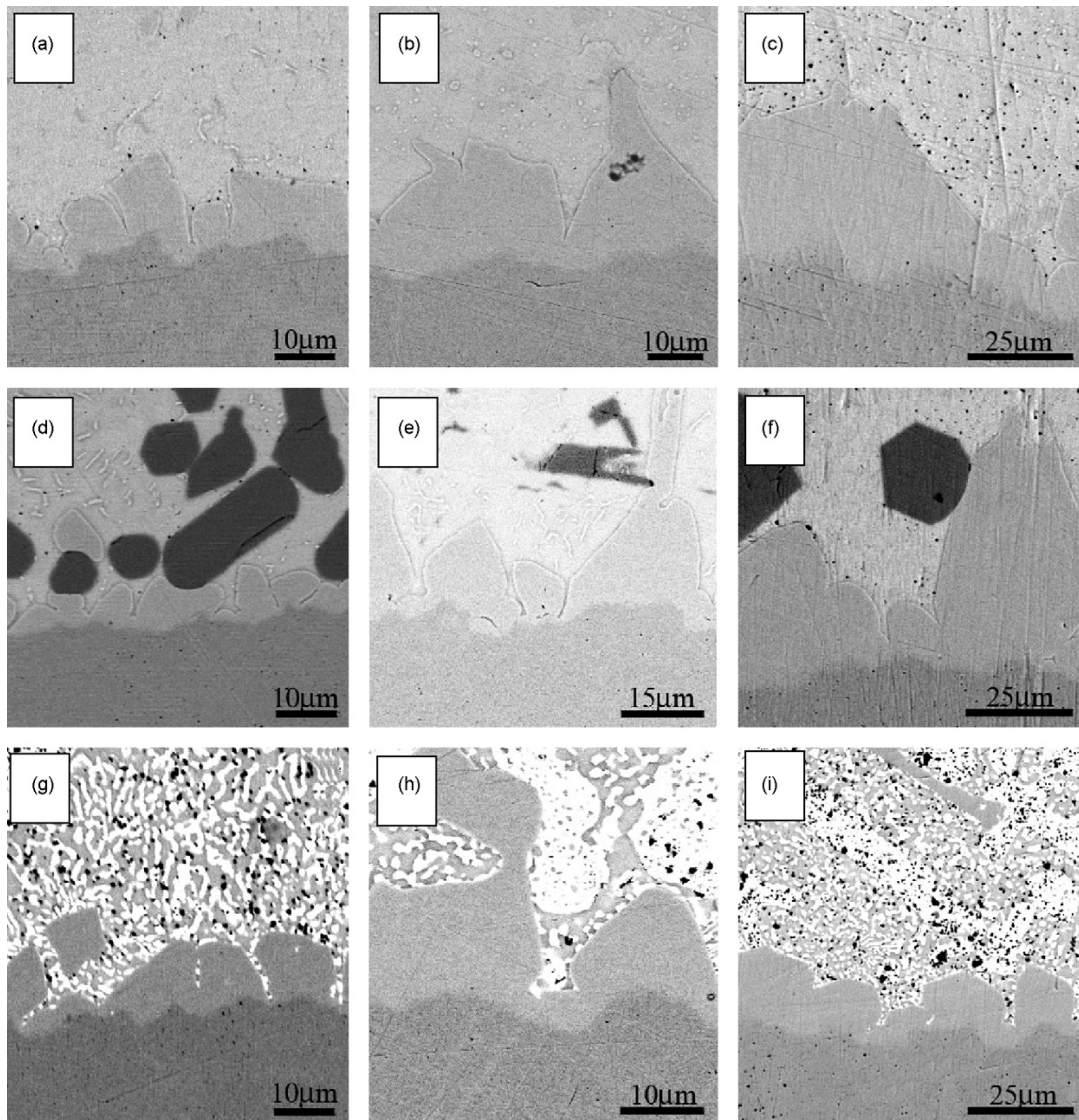

Fig. 4. SEM micrographs of the Ag_3Sn IMC between the three solders and single crystal Ag substrate after aging at 260 °C for different hours: (a) 0.5 h, (b) 1.5 h, (c) 9 h for Sn–4Ag/Ag; (d) 0.5 h, (e) 1.5 h, (f) 9 h for Sn–3Cu/Ag; (g) 0.5 h, (h) 1.5 h, (i) 9 h for Sn–37Pb/Ag.

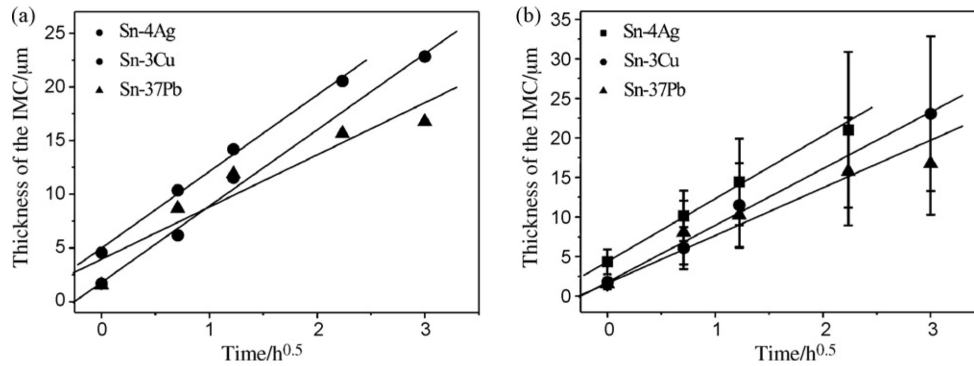

Fig. 5. Plot of the thickness of the Ag_3Sn layer vs. the square root of aging hours for different solders at 260 °C: (a) method I; (b) method II.

a decreasing order, i.e. $[Ag]_{Sn\text{–}4Ag} > [Ag]_{Sn\text{–}3Cu} \geq [Ag]_{Sn\text{–}37Pb}$. According to Eq. (7), the order of ΔG for different samples should be: $\Delta G_{Sn\text{–}4Ag} < \Delta G_{Sn\text{–}3Cu} \leq \Delta G_{Sn\text{–}37Pb}$. According to thermodynamics, it predicts a different initial IMC thickness for the as-reflowed samples with a decreasing order of $T_{Sn\text{–}4Ag} > T_{Sn\text{–}3Cu} \geq T_{Sn\text{–}37Pb}$, which is confirmed by the as-reflowed results for the three solders, as shown in Figs. 1(a), (d) and (g) and 3.

However, during solid-state aging of the three solder joints at the same temperature, all the Ag and Sn atoms for growth of the IMC layer have to move through the same phase—Ag_3Sn, which results in the nearly same diffusion coefficients for the different solders. Therefore, it is not difficult to understand why the slopes of the growth lines are approximately equal for the three different solders with the same substrate (Ag) during the solid-state aging at 160 °C.

3.2. The liquid-state interfacial reaction

Fig. 4 shows SEM micrographs for the interfaces between Sn–4Ag, Sn–3Cu and Sn–37Pb solders and single crystal Ag substrate after liquid-state aging at 260 °C for different periods. Thick IMC layer was detected, and its thickness is proportional to the square root of the reaction time, as shown in Fig. 5. This indicates that the interfacial reaction is still diffusion-controlled during liquid-state aging. From Eq. (3) and the data in Fig. 5, the diffusion coefficients of Ag and Sn atoms were calculated to be 1.41×10^{-14}, 1.39×10^{-14}, and $0.66 \times 10^{-14}\,m^2\,s^{-1}$ for Sn–4Ag, Sn–3Cu and Sn–37Pb solders, respectively (1.74×10^{-14}, 1.35×10^{-14}, and $1.0 \times 10^{-14}\,m^2\,s^{-1}$ for method II). Compared with Fig. 3(b), the data in Fig. 5(b) is more scatter. The diffusion coefficients for liquid-state aging are about three orders of magnitude higher than those for solid-state aging. The results are less than those for Sn–9Zn–0.5Ag/Cu ($5.76 \times 10^{-14}\,m^2\,s^{-1}$) and Sn–9Zn–1.5Ag/Cu ($2.82 \times 10^{-14}\,m^2\,s^{-1}$) solder joints aging at 250 °C, respectively [24], but higher than those of Sn–3.5Ag/Ni ($0.6 \times 10^{-14}\,m^2\,s^{-1}$) and Sn–37Pb/Ni ($0.39 \times 10^{-14}\,m^2\,s^{-1}$) solder joints at 260 °C, respectively [25]. These results further indicate that the diffusion coefficients of the solders through the IMCs are more dependent on the substrates, which is discussed below.

Based on the observations from the solid-state and liquid-state aging experiments, there are some differences in the diffusion coefficient and the growth thickness of IMCs between the three different solder joints. For solid-state aging, the diffusion coefficients of the three joint samples are nearly the same, but there are some differences for the liquid-state aging especially for Sn–37Pb. This can be understood using Eq. (7) and phase diagrams. In other words, the difference in the solubility or concentration of Ag atoms in the three solders leads to different growth rates of IMC layers. With increasing aging time under liquid-state aging, the equilibrium concentrations of Ag atoms in Sn–3Cu and Sn–4Ag alloys at 260 °C were calculated to be about 6 and 7 wt% from the previous phase diagrams [2,26], respectively. So the order of [Ag] for the aged samples in the three solders follows $[Ag]_{Sn\text{–}4Ag} \geq [Ag]_{Sn\text{–}3Cu} > [Ag]_{Sn\text{–}37Pb}$. Therefore, with increasing aging time, the growth rate of IMCs in the Sn–3Cu/Ag joint is still similar to that of Sn–4Ag/Ag joint because the solubility of Ag is approximately equal for the two solders.

It can be observed in Fig. 6 that there are many flaky Ag_3Sn IMCs in Sn–4Ag and Sn–3Cu solders; however, for Sn–37Pb solder, there are no flaky Ag_3Sn or Ag_3Sn particles, but a few planar-type or other type Ag_3Sn exists in the solder. In particular, the density of the flaky Ag_3Sn IMC in the Sn–3Cu solder increases with increasing aging time, as clearly observed in Fig. 6(c) and (d). Therefore, based on the quantity of Ag_3Sn near the interface, it can be concluded that the order of the concentrations of Ag in the three solders is $[Ag]_{Sn\text{–}4Ag} \geq [Ag]_{Sn\text{–}3Cu} > [Ag]_{Sn\text{–}37Pb}$.

3.3. Inner-crack analysis

Fig. 7 displays the microstructures of Sn–3Cu/Ag and Sn–4Ag/Ag joints after aging at different temperatures. According to Figs. 1, 4, 7(c) and (d), it can be seen that there is no local crack in the joints of Sn–Pb and Sn–Ag solders with Ag substrate when the samples were aged for many days. For Sn–3Cu/Ag solder joint, however, it is clear to see that a local crack has initiated along the interface between Sn–3Cu/IMC when the aging time increases to 11 days during solid-state aging at 160 °C, as indicated by the arrow in Fig. 7(a). When the aging time increases to 15 days, in addition to the interfacial cracks, many other small cracks were observed within the Cu_6Sn_5 particles in the Sn–3Cu

solder when the particle size is less than 10 μm, as indicated by the arrow in Fig. 7(b). Such behavior was also detected previously for many Sn-based solders on Cu substrates [27–30], as a common sense, those cracks should dramatically deteriorate the mechanical properties of the solder joints. Such cracking was not observed for the Sn–37Pb/Ag and Sn–4Ag/Ag joints under the same aging condition. Meanwhile, for the Sn–3Cu solder, when the sample was subjected to high-temperature reflowing for many hours, there is no crack in the Cu_6Sn_5 particles or the interface between Sn–3Cu/IMC even though its dimension is above 50 μm, as displayed in Fig. 7(c).

Based on the observations above, there might be some explanations for the difference in the formation of local cracking in different solders or near the interfaces. Firstly, it may be that the difference in thermal expansion coefficient between Ag and Ag_3Sn is smaller than that between Cu and Cu–Sn IMCs. As a result, it causes higher local stress between the Cu–Sn IMC and Cu substrate during solid-state aging. In addition, it is known that the Young's modulus of Cu_6Sn_5 and Ag_3Sn are 112.3 and 78.9 GPa, respectively [31]. However, there is little difference in the Young's modulus between solders. For example, the Young's modulus of the Sn–3Ag and Sn–37Pb are 50 and 39 GPa, respectively [1]. As a result, the difference in the Young's modulus between the Sn–Cu solder and Cu_6Sn_5 is greater than that between the Sn–Pb and Sn–Ag solders and Ag_3Sn. The larger difference in their Young's modulus should lead to a higher stress concentration near the interface or between the solder and the Cu_6Sn_5 phase [27]. Therefore, the Cu atom might be prevented from diffusing into the solder for the increasing stress concentration with increasing aging time. Meanwhile, compared with solid-state aging, the resistance to coarsen the Cu_6Sn_5 is smaller during the liquid-state aging because Cu_6Sn_5 grains are embedded in the liquid-state solder. In this case, there is no internal stress during the liquid-state aging. In contrast, the resistance for coarsening the Cu_6Sn_5 grains should be higher under the solid-state aging because the Cu_6Sn_5 grains are embedded by the solid-state solder rather than by the liquid-state solder. Finally, there might be some differences in the physical and mechanical properties between Cu_6Sn_5 and Ag_3Sn, for example, Ag_3Sn is softer and more ductile than Cu–Sn IMCs [31,32]. Altogether, Cu_6Sn_5 and Ag_3Sn IMCs are two important production phases after aging of various solder joints, the observations above give

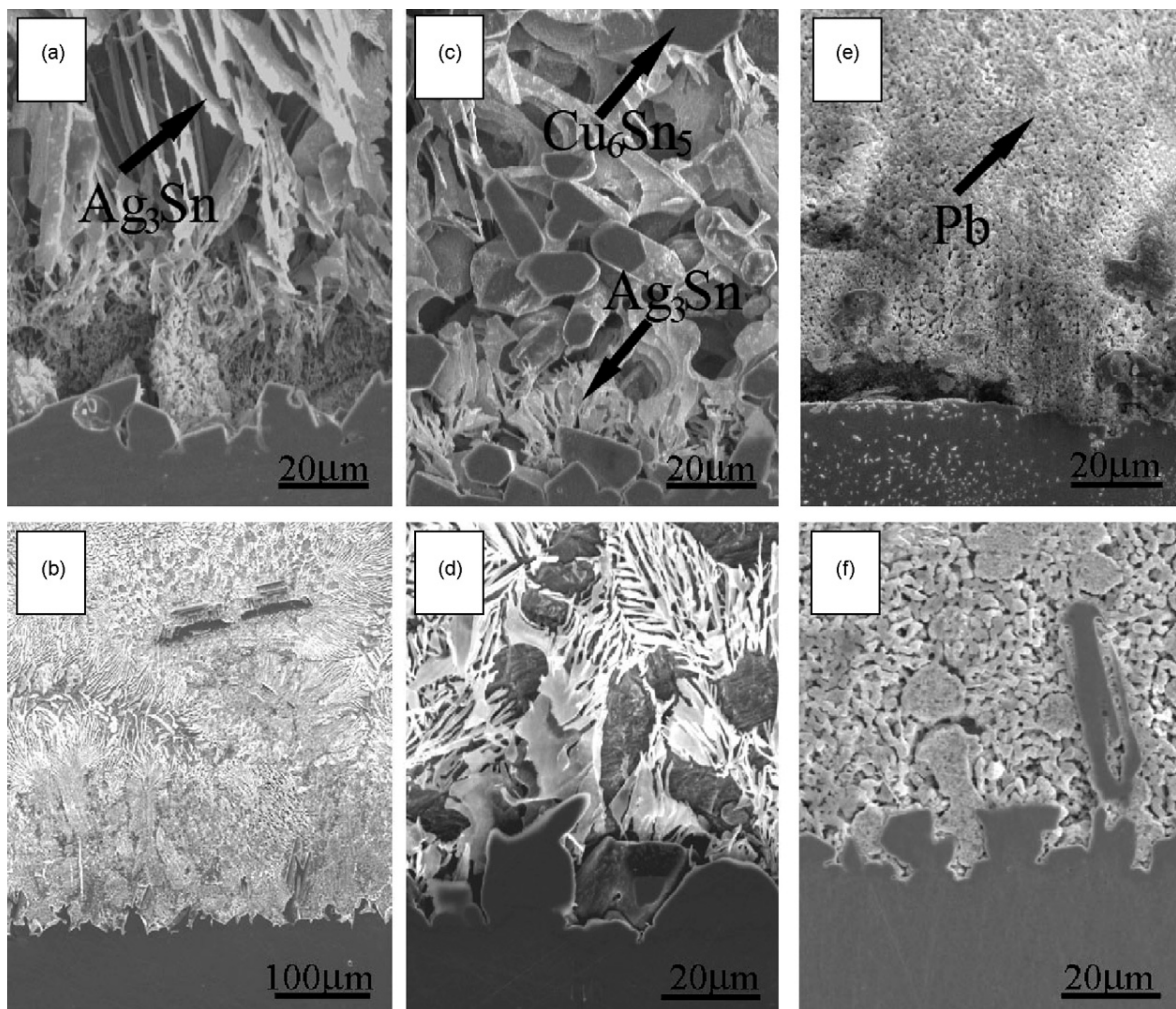

Fig. 6. Cross-sectional images of the interfaces at 260 °C by deep erosion: (a) 0.5 h and (b) 1.5 h for Sn–4Ag/Ag; (c) 0.5 h and (d) 1.5 h for Sn–3Cu/Ag; (e) 0.5 h and (f) 1.5 h for Sn–37Pb/Ag.

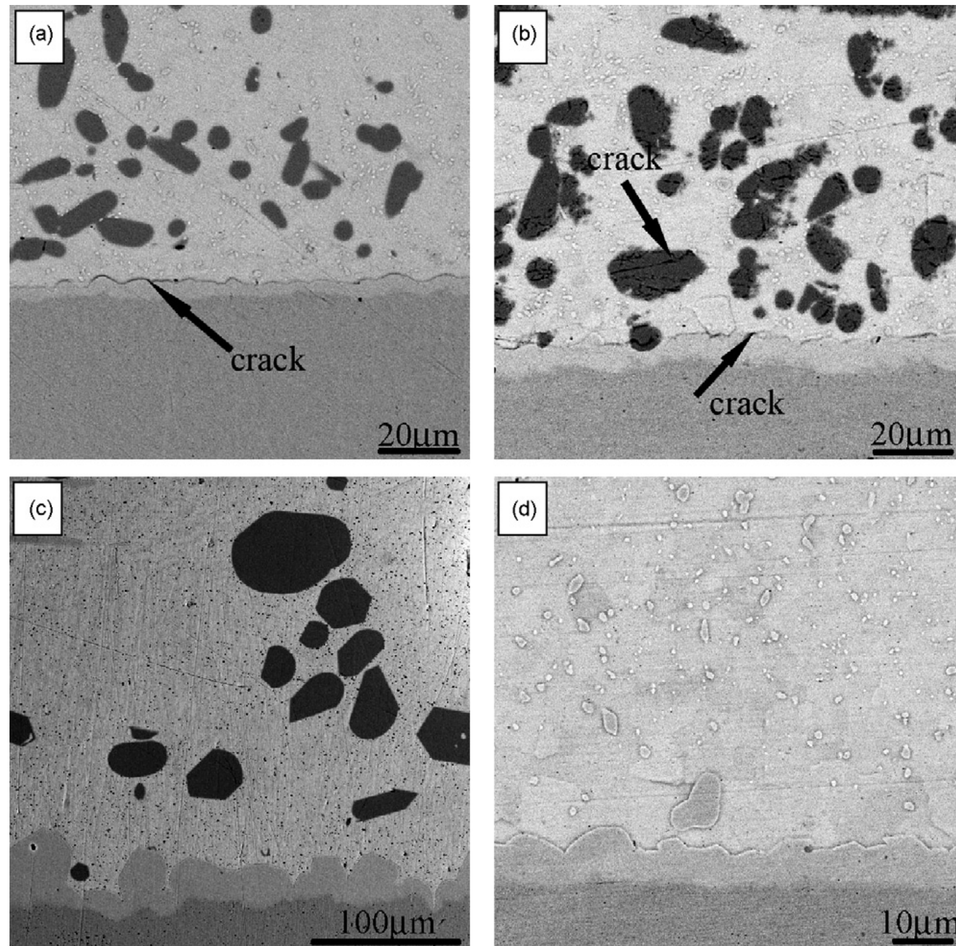

Fig. 7. Sn–3Cu/Ag joint aging for: (a) 11 days at 160 °C, (b) 15 days at 160 °C, and (c) 9 h at 260 °C; (d) Sn–4Ag/Ag joint aging for 15 days at 160 °C.

rise to an interesting question to the electronic packaging field, which will be further investigated elsewhere.

4. Conclusions

In this study, the solid-state and liquid-state interfacial reactions between Sn–4Ag, Sn–3Cu and Sn–37Pb solders and single crystal Ag substrate were studied and the following conclusions can be drawn.

Under the solid-state aging condition, the thicknesses of IMC in the as-reflowed samples are different for the three solders. But their IMC growth rates are nearly the same under the same aging temperature. The measured diffusion coefficients of Ag and Sn atoms are: 0.98×10^{-17}, 2.15×10^{-17}, and $1.12 \times 10^{-17}\,m^2\,s^{-1}$, for Sn–4Ag, Sn–3Cu, and Sn–63Pb solders, respectively.

Under the liquid-state aging condition, the growth rates of IMCs displayed certain difference for the three solders under the same aging temperature. The values of the diffusion coefficient are calculated to be: 1.41×10^{-14}, 1.39×10^{-14}, and $0.66 \times 10^{-14}\,m^2\,s^{-1}$, for Sn–4Ag, Sn–3Cu, and Sn–37Pb, respectively.

When the Cu_6Sn_5 particles appear in the solder or near the interface, it is frequently found that small cracks appear at the interface or around the Cu_6Sn_5 particles during solid-state aging. Those cracks would deteriorate the mechanical properties of the soldering joints, it is suggested that Ag is a better substrate than Cu because the Cu_6Sn_5 particles can be avoided between the Sn-based solder and Ag substrate.

Acknowledgements

The authors would like to thank W. Gao, H.H. Su, J.X. Hu, J.T. Fan, Q.S. Zhu and Q.Q. Duan for the sample preparation, SEM observations, and Dr. F. Yang for his careful corrections on the revised manuscript. This work was financially supported by National Basic Research Program of China under Grant No. 2004CB619306 and National Outstanding Young Scientist Foundation under Grant No. 50625103.

References

[1] M. Abtew, G. Selvaduray, Mater. Sci. Eng. R 27 (2000) 95.
[2] T. Lauril, V. Vuorinen, J.K. Kivilahti, Mater. Sci. Eng. R 49 (2005) 1.
[3] C.H. Wang, S.W. Chen, Acta Mater. 54 (2006) 247.
[4] J. Gong, C.Q. Liu, P.P. Conway, V.V. Silberschmidt, Mater. Sci. Eng. A 427 (2006) 60.
[5] P. Sun, C. Andersson, X.C. Wei, Z.N. Cheng, D.K.S. Guan, J. Liu, J. Alloys Compd. 425 (2006) 191.

[6] F.Y. Hung, C.J. Wang, S.M. Huang, L.H. Chen, T.S. Lui, J. Alloys Compd. 420 (2006) 193.
[7] K.I. Chen, S.C. Cheng, S. Wu, K.L. Lin, J. Alloys Compd. 416 (2006) 98.
[8] J.F. Li, S.H. Mannan, M.P. Clode, K. Chen, D.C. Whalley, C. Liu, D.A. Hutt, Acta Mater. 55 (2007) 737.
[9] J.F. Li, S.H. Mannan, M.P. Clode, D.C. Whalley, D.A. Hutt, Acta Mater. 54 (2006) 2907.
[10] X.Q. Wei, H.Z. Huang, L. Zhou, M. Zhang, X.D. Liu, Mater. Lett. 61 (2007) 655.
[11] E. Saiz, C.W. Hwang, K. Suganuma, A.P. Tomsia, Acta Mater. 51 (2003) 3185.
[12] B.J. Lee, N.M. Hwang, H.M. Lee, Acta Mater. 45 (1997) 1867.
[13] J.W. Yoon, S.W. Kim, S.B. Jung, J. Alloys Compd. 415 (2006) 56.
[14] Y.H. Lee, H.T. Lee, Mater. Sci. Eng. A 444 (2007) 75.
[15] F.J. Wang, X. Ma, Y.Y. Qian, Scripta Mater. 53 (2005) 699.
[16] H.F. Hsu, S.W. Chen, Acta Mater. 52 (2004) 2541.
[17] C.-M. Chen, K.-J. Wang, K.-C. Chen, J. Alloys Compd. 432 (1–2) (2007) 122.
[18] Y.T. Huang, T.H. Chuang, Z. Metallkd. 12 (2000) 1002.
[19] M.D. Cheng, S.S. Wang, T.H. Chuang, J. Electron Mater. 31 (3) (2002) 171.
[20] P.Y. Yeh, J.M. Song, K.L. Lin, J. Electron Mater. 35 (3) (2006) 978.
[21] Q.S. Zhu, Z.F. Zhang, J.K. Shang, Z.G. Wang, Mater. Sci. Eng. A 435–436 (2006) 588.
[22] X. Ma, F.J. Wang, Y.Y. Qian, F. Yoshida, Mater. Lett. 57 (2003) 3361.
[23] C.H.P. Lupis, Chemical Thermodynamics of Materials, Elsevier Science Publishing Co. Inc., New York, 1983, p. 116.
[24] T.-C. Chang, M.-C. Wang, M.-H. Hon, J. Crystallogr. Growth 252 (2003) 401.
[25] C.-Y. Lin, C.-C. Jao, C. Lee, Y.-W. Yen, J. Alloys Compd. 440 (1–2) (2007) 333.
[26] K. Zeng, K.N. Tu, Mater. Sci. Eng. R 38 (2002) 55.
[27] H.-T. Lee, M.-H. Chen, Mater. Sci. Eng. A 333 (2002) 24.
[28] M.N. Islam, Y.C. Chan, A. Sharif, M.J. Rizvi, J. Alloys Compd. 396 (2005) 217.
[29] M.J. Rizvi, Y.C. Chan, C. Bailey, H. Lub, M.N. Islam, J. Alloys Compd. 407 (2006) 208.
[30] A. Sharif, Y.C. Chan, J. Alloys Compd. 393 (2005) 135.
[31] X. Deng, M. Koopman, N. Chawla, K.K. Chawl, Mater. Sci. Eng. A 364 (2004) 240.
[32] P.R. Chromik, R.P. Vinci, S.L. Allen, M.R. Notis, J. Mater. Res. 18 (9) (2003) 2251.